# Detergent free purification of ABC transporters

Sonali Gulati[*], Mohammed Jamshad[†], Timothy J. Knowles[‡], Kerrie A. Morrison[*], Rebecca Downing[*], Natasha Cant[§], Richard Collins[§], Jan B. Koenderink[‖], Robert C. Ford[§], Michael Overduin[‡], Ian D. Kerr[¶], Timothy R. Dafforn[†] & Alice J. Rothnie[*]

[*]School of Life & Health Sciences, Aston University, Aston Triangle, Birmingham, B4 7ET, UK

[†]School of Biosciences, University of Birmingham, Edgbaston, Birmingham, B15 2TT, UK

[‡]School of Cancer Studies, University of Birmingham, Edgbaston, Birmingham, B15 2TT, UK

[§]Faculty of Life Sciences, University of Manchester, Manchester, M13 9PT,

[‖]Department of Pharmacology and Toxicology, Radboud University Nijmegen Medical Centre, Nijmegen Centre for Molecular Life Sciences, The Netherlands.

[¶]School of Life Sciences, University of Nottingham Medical School, Queen's Medical Centre, Nottingham, UK

Corresponding author: Dr Alice Rothnie, School of Life & Health Sciences, Aston University, Aston Triangle, Birmingham, B4 7ET, UK. a.rothnie@aston.ac.uk
Tel. +44 (0)121 204 4013

Abstract:

ABC (ATP Binding Cassette) transporters carry out many vital functions and are involved in numerous diseases, but study of the structure and function of these proteins is often hampered by their large size and membrane location. Membrane protein purification usually utilises detergents to solubilise the protein from the membrane, effectively removing it from its native lipid environment. Subsequently lipids have to be added back and detergent removed to reconstitute the protein into a lipid bilayer. We present here the application of a new methodology for the extraction and purification of ABC transporters without the use of detergent, instead using a styrene maleic acid co-polymer (SMA). SMA inserts in a bilayer and assembles into discrete particles, essentially solubilising the membrane into small discs of bilayer encircled by polymer, termed SMA lipid particles (SMALPs). We show that this polymer can extract several eukaryotic ABC transporters; P-glycoprotein (ABCB1), MRP1 (ABCC1), MRP4 (ABCC4), ABCG2 and CFTR (ABCC7), from a range of different expression systems. The SMALP encapsulated ABC transporters can be purified by affinity chromatography, and are able to bind ligands comparably to those in native membranes or detergent micelles. A greater degree of purity and enhanced stability is seen compared to detergent solubilisation. This study demonstrates that eukaryotic ABC transporters can be extracted and purified without ever being removed from their lipid bilayer environment, opening up a wide range of possibilities for the future study of their structure and function.

Summary statement:

A styrene maleic acid copolymer can be effectively used to extract and purify large eukaryotic transmembrane proteins in the absence of detergents, forming small bilayer discs encapsulating the protein, which have great potential for future structure & function studies.

Short title: Detergent free purification of ABC transporters

Keywords: membrane protein, solubilisation, purification, polymer, nanodisc, detergent

Introduction:

The ABC (ATP Binding Cassette) transporter superfamily is found in all organisms from bacteria to man, with humans possessing 48 different members [1]. The human transporters are involved in a wide range of functions within the body including protection from toxins, metabolism, controlling drug distribution in the body, mediating inflammatory responses and transporting lipids [2-5]. Several members are involved in causing drug resistance during cancer treatment [6], while others are responsible for genetic diseases such as cystic fibrosis and adrenoleukodystrophy [7, 8].

The study of the function and structure of these vital proteins is often hampered by difficulties in expressing, extracting and purifying them, as they are large transmembrane proteins requiring a lipid bilayer environment. Traditionally purification of membrane proteins such as these has used detergent to solubilise the protein from the membrane, thus removing it from its native lipid environment. Following purification lipids need to be added back in and detergent removed to reconstitute the protein into a lipid bilayer [9]. These reconstituted systems include proteoliposomes and planar membranes, and more recently several forms of lipid nano-particles, such as bicelles or nanodiscs. The last of these, nanodiscs use membrane associated amphipathic peptides to produce small discs of membrane bilayer into which membrane proteins can be inserted [10]. Several ABC transporters have been successfully incorporated into nanodiscs, to enable many downstream applications [11-14]. However formation of these particles still requires detergent solubilisation of the protein before reconstitution into the nanodiscs. Detergent solubilisation requires an expensive, trial and error process, and detergents that work well for solubilisation may not be compatible with downstream purification or analytical methods [15, 16].

Here we report the application of a recently developed system for detergent-free extraction of ABC transporters from their native membranes using a readily available, biocompatible and chemically stable polymer, polystyrene-co-maleic acid (SMA) [17-19]. The polymer inserts into the membrane isolating small discs of lipid bilayer that are encircled by the polymer, termed SMA lipid particles (SMALPs) [17]. We demonstrate that the polymer is able to effectively solubilise several different eukaryotic ABC transporters from a range of different cell types, including mammalian cells, insect cells and yeast. ABC transporters within the SMALPs can then be purified using standard affinity chromatography methods. We demonstrate that the proteins within the SMALPs can bind substrates comparably to those in native membranes or detergent micelles, and we characterise the biophysical properties of a SMALP-purified transporter.
Overall this study demonstrates that the SMALP method can be successfully applied to eukaryotic ABC transporters to extract and purify them without ever removing them from their lipid environment.

Experimental:

*SMA preparation*

SMA polymer was prepared as described previously [17]. Briefly, a 10% (w/v) solution of SMA copolymer in 1M NaOH was refluxed for 2 hours, allowed to cool to room temperature, then dialysed against 20mM Tris buffer pH8 before use.

*Cell culture, expression & membrane preparation*

High Five (*Trichoplusia ni*) insect cells were cultured and infected with recombinant baculovirus to express either human P-glycoprotein (Pgp/ABCB1) with a C-terminal 12-His tag or human ABCG2 with an N-terminal 6-His-tag, and membrane preparations carried out as described previously [15, 20]. Murine CFTR (cystic fibrosis transmembrane regulator/ABCC7) with two hexa-histidine tags and a GFP tag was expressed in *Sacchromyces cerevisiae* and microsomes prepared as described elsewhere [21]. MRP1 (ABCC1) overexpressing drug selected H69AR small cell lung cancer cell line was cultured as described previously [22]. MRP1 was also expressed in HEK cells by transfection of the pcDNA3.1-MRP1 plasmid [23] using JetPRIME transfection reagent (Polyplus-transfection). Plates (10cm) were seeded with $1.3x10^6$ cells transfected after 24 hours with 10µg DNA/plate and 20µl JetPRIME/plate, and harvested 48 hours later. ABCG2 was expressed in either MCF7-FLV cells cultured as described [24], or following transfection of HEK293T cells with pcDNA3.1_His6_ABCG2 [25]. MRP4 (ABCC4) with a C-terminal hexa-histidine tag was expressed in HEK cells and membranes prepared as described before [26]. MRP4 with a C-terminal hexa-histidine tag was also expressed in *Spodoptera frugiperda* (Sf9) insect cells by infection with a recombinant baculovirus. The cDNA for MRP4 was amplified from the pcDNA3.1-MRP4 plasmid [27], and the stop codon mutated to an AgeI site by PCR (using the following primers 5' ctacgtcgacgacctaggcatgctgcccg and 3' ctaagatttagtcgcggccgctcaatggtgatg). The PCR product was digested with EcoRI and AgeI and subcloned into a pFastBac-1 vector, resulting in the generation of a C-terminally hexahistidine tagged construct. Recombinant baculovirus was formed using the Bac-to-Bac kit (Invitrogen). Sf9 cells were maintained at $0.5–2.5×10^6$ cells/mL in shaker cultures at 28 °C in Insect Xpress media (Lonza) supplemented with 10% (v/v) fetal bovine serum, 100 U/mL penicillin, and 100 mg/mL streptomycin. MRP4 expressing baculovirus was amplified by infection of Sf9 cells ($1×10^6$ cells/mL) at a multiplicity of infection (MOI) of 0.2 for 5 days. MRP4 expression in Sf9 cells was achieved by infection with the baculovirus at an MOI of 5 for 3 days. Cells were harvested by centrifugation (6000 g, 20 min, 4°C). Whole cell pellets of MCF7-FLV, HEK293T-ABCG2, H69AR, HEK-MRP1 or Sf9-MRP4 were resuspended in buffer 1 (50 mM Tris pH7.4, 250 mM sucrose) supplemented with 0.25 mM $CaCl_2$ and protease inhibitors (Roche or Pierce), then lysed by nitrogen cavitation (500 psi, 15 min, 4°C). Cell debris was removed by low speed centrifugation (750 g, 20 min, 4°C), then membranes were harvested by ultracentrifugation (100000 g, 20 min, 4°C). Membranes were resuspended in buffer 1, aliquoted and stored at -70°C for up to 6 months.

*SMA extraction*

Membranes were pelleted (100000 g, 20 min, 4°C ) then resuspended in buffer 2 (20 mM Tris pH8, 150 mM NaCl, 20% (v/v) glycerol) at a final concentration of 30 mg/ml membrane (wet membrane weight) and SMA was then added to a final concentration of 2.5% (w/v). Samples were incubated at room temperature with gentle shaking for 30 - 60 minutes. Insoluble material was removed by centrifugation (100000 g, 20 min, 4°C). For ABCG2 from High Five insect cells only, this method was modified slightly in that 1% (w/v) DMPC was also included alongside the SMA, the sample was briefly probe sonicated and incubated at 37°C.

The insoluble pellet was resuspended in buffer containing 2.5% SDS (w/v) to the same volume as the soluble fraction. Samples of both the soluble and insoluble fractions were analysed by Western blotting. For most of the proteins studied an anti-His primary antibody was used (R & D Systems, typically at 1:500 dilution). For the H69AR samples the primary antibody used was QCRL-1 (1:2000). For the MCF7-FLV and HEK-ABCG2 samples the primary antibody was Bxp-21 (Merck 1:2000). In all cases either an anti mouse-Alkaline Phosphatase (Sigma) or anti mouse-HRP (Sigma) secondary antibody was used, and visualised using BCIP/NBT colorimetric detection (Sigma) or chemiluminescence (Pierce) respectively. The efficiency of solubilisation was quantified from the Western blots using densitometry (Image J).

*$Ni^{2+}$-NTA affinity purification*

SMA-solubilised membranes were incubated overnight at 4°C with $Ni^{2+}$-NTA agarose (Qiagen) using 100 µl resin/ml solubilised membrane and slowly rotated. The sample was transferred to a gravity flow column (Biorad), washed 5 times with 10 bed volumes (bv) of buffer 2 supplemented with 20 mM imidazole, then twice with 10 bv of buffer 2 supplemented with 40 mM imidazole, then once with 2 bv of buffer 2 supplemented with 60 mM imidazole. Proteins were eluted using buffer 2 supplemented with 120 mM imidazole and 1 bv fractions were collected. Samples of various stages of the purification were analysed by SDS-PAGE and visualised by silver staining (Pierce). The concentration of purified proteins were determined using Coomassie stained SDS-PAGE gels as described previously (Rothnie et al 2004 JBC).

Following purification, samples were concentrated and/or buffer exchanged using centrifugal concentrators (Amicon Ultra, Millipore, 30000 MWCO) or subjected to gel filtration spin columns to remove imidazole (Biorad, Micro Bio-Spin columns).

*Protein A and antibody affinity purification*

Immunoaffinity purification of MRP1 from H69AR membranes using the monoclonal antibody QCRL-1 was based on the procedure of Mao *et al* [28]. Briefly, QCRL-1 ascites fluid (50 µl) was diluted to 1ml in buffer 2, then slowly injected on to a protein A AcroSep pre-packed 1ml column (PALL). After incubation at room temperature for 30 min the column was washed 10 x 1 ml with buffer 2. SMALP-encapsulated H69AR membranes (1 ml) were then slowly injected on to the column. After 30 mins the column was washed 10 x 1 ml with buffer 2. MRP1 was eluted from the column using buffer 2 supplemented with the peptide SSYSGDI (ThermoFisher Custom Biopolymers) at 3.3 mg/ml, and 1 ml fractions were collected.

*Drug binding to Pgp: Fluorescence quenching assay*

Formation of the Pgp:drug complex was studied using the fluorescence quenching method of Liu and Sharom [29]. In this method the fluorophore, MIANS, was first used to label cysteine residues within the two nucleotide binding domains of ABC transporters. Purified Pgp (100 µg/mL) encapsulated within SMALPs was incubated with 20 µM MIANS (Invitrogen) at room temperature for 1 h in the dark. DTT (1 mM) was added to quench unreacted fluorophore. Separation of MIANS-labelled Pgp-SMALPs from DTT-MIANS was performed by gel filtration chromatography on Micro Bio-Spin columns (Bio-rad). Fluorescence quenching of MIANS-labelled Pgp-SMALP (50 µg/mL) by successive additions of doxorubicin (2.5-25 µM) or verapamil (0.5-12 µM) was measured using a Perkin Elmer LS55 fluorimeter at an excitation wavelength of 322±10 nm and emission wavelength of 420 nm (λmax). Fluorescence intensities were corrected for dilution, scattering and inner filter effect as described previously [29]. Results were analysed by non-linear regression using Graphpad Prism (Graphpad Software Inc.) to fit a one-site binding hyperbolic equation 1:

$B = B_{max}.[L]/(K_d + [L])$

*Drug binding to MRP1: Radioligand binding assay*

The binding of 40 nM $^3$H-estrone sulphate (Perkin Elmer) to SMALP encapsulated membranes from H69AR cells, in the presence or absence of 3 mM GSH was performed as described previously [30]. However instead of using rapid filtration to separate bound and unbound radioligand, samples were instead loaded onto pre-equilibrated Micro Bio-Spin columns (Biorad) and the void volumes collected by centrifugation (3000 rpm, 4 min). Scintillation counting was performed using a Packard Tri-Carb Liquid Scintillation counter.

Statistical analysis used a student t-test (GraphPad Prism), and a $P<0.05$ was considered significant.

*Drug binding to ABCG2: Pheophorbide A fluorescence*

Binding of SMALP encapsulated ABCG2 to the fluorescent substrate pheophorbide A was detected by an enhancement of the fluorescence intensity. Pheophorbide A (10 µM, 1 ml) fluorescence emission spectra (640 – 720 nm) were measured at an excitation wavelength of 390±10 nm using a Perkin Elmer LS55 fluorimeter. Successive additions (5 – 100 µl) of SMALP encapsulated membranes from cells overexpressing ABCG2 were added to the pheophorbide A and incubated for 10 minutes before reading the fluorescence spectra again. Specific binding to ABCG2 was determined by subtracting the fluorescence intensity obtained when membranes lacking ABCG2 were added to pheophorbide A, or the ABCG2 membranes were pre-incubated with chrysin (30 µM) for 10 minutes before addition to pheophorbide A. Results were analysed by non-linear regression using Graphpad Prism (Graphpad Software Inc.) to fit equation 1.

*Nucleotide binding to Pgp; tryptophan fluorescence quenching*

Binding of nucleotides to purified Pgp within SMALPs was assayed by measuring the quenching of intrinsic tryptophan fluorescence as described previously [31]. Briefly, the fluorescence of purified Pgp (50 µg/mL) encapsulated within SMALPs was measured using a Perkin Elmer LS55 fluorimeter at an excitation wavelength of 290±10 nm and emission wavelength of 330 nm (λmax), and the quenching by successive additions of ATP (0.05-2 mM) or the non-hydrolysable fluorescent ATP analog, TNP-ATP (9.8-160 µM) was measured. Fluorescence intensities were corrected for dilution, scattering and inner filter effect as described previously [29]. Results were analysed by non-linear regression using Graphpad Prism (Graphpad Software Inc.) to fit a one-site binding hyperbolic (equation 1).

*Circular Dichroism Spectroscopy*

Purified Pgp within SMALPs was buffer exchanged into 10 mM Tris pH 8 and concentrated to 0.65 mg/ml. The circular dichroism spectra was measured using a JASCO J-715 CD spectrophotometer with a path length of 0.1 cm at room temperature. The sample was scanned 8 times at 200 nm/min with a bandwidth of 2 nm. A spectrum of the buffer used in the experiment was used as a background.

*Analytical Ultracentrifugation*

Purified Pgp encapsulated within SMALPs (0.65 mg/ml) in 10 mM Tris pH 8 was subjected to analysis using sedimentation velocity analytical ultracentrifugation. The sample was centrifuged at 40000 rpm/129000g at 4$^o$C in a Ti50 rotor within a Beckman XL-1 analytical ultracentrifuge (Beckman 693 Coulter, Palo Alto, CA, USA). The movement of the protein within the cell was monitored using absorbance at 280 nm with 1780 datasets (890 each for absorbance and velocity)

being collected over 23 hr 22 min. These data were analysed using SEDFIT [32] and the c(s) and c(M) method. Values for Vbar and buffer viscosity and density were calculated using SEDNTERP [33].

*Gel filtration*

Purified Pgp encapsulated within SMALPs was run on a Superdex 200 gel filtration column (diameter 1.6 cm, column height 55 cm) pre-equilibrated in 20 mM Tris pH8 using an AKTA Purifier system. A total of 50 µg in a volume of 0.5 ml 20 mM Tris pH 8 was loaded and the column was run at a flow rate of 0.5 ml/min. The column was calibrated using the following standards: Blue Dextran, Bovine Serum Albumin, Carbonic Anhydrase, Cytochrome c and Aprotinin (Sigma).

*Electron microscopy*

Holey electron microscopy grids (2micron holes, Quantifoil) were prepared of purified Pgp encapsulated within SMALPs (1 mg/ml) using an FEI Vitrobot freezing device with plunge freezing into liquid ethane. Grids were transferred into a Polara FEG transmission electron microscope and maintained at <100K throughout. Areas with sufficiently thin ice were selected at low magnification and low dose, and then micrographs were recorded on a 4k x 4k CCD device with 1 sec exposure and low dose mode imaging conditions. Micrographs were analysed using the EMAN2 software package [34], with >8000 particles selected from 20 images. Strong defocus was employed because of the relatively small mass of the particles (defocus range 3.5 to 5.9 micron). Correction for the contrast transfer function was carried out and then reference-free classification of the particles was performed with unique 32 classes identified. Preliminary 3D structures were generated from these classes using a common-lines algorithm and with no symmetry applied. The ten low resolution structures were similar and one was selected for refinement of the 3D structure using all the single particles. The resolution of the structure after 5 rounds of refinement was estimated by Fourier shell correlation between two structures generated from even- and odd-numbered particles from the data set. The features observed in the final structure corresponded to the resolution estimate and with the strong suppression of higher resolution frequencies in the images as a result of the need for strong underfocus.

Thermostability

Pgp was extracted from High Five membranes either using 2.5% (w/v) SMA as described above or 2% (w/v) octyl-glucoside plus 0.4% (w/v) lipids (4:1 *E.coli* lipid extract:cholesterol) as detailed in [20], then purified by Ni-NTA affinity chromatography as described above, except supplementing the buffers with 1.25% (w/v) octyl-glucoside and 0.1% (w/v) lipids. Relative thermostability of the purified proteins was monitored using the thiol-reactive flourophore 7-diethylamino-3-(4-maleimidophenyl)-4-methylcoumarin (CPM, Sigma) as described by Alexandrov *et al* [35]. CPM is essentially non-fluorescent until it reacts with a sulphydryl, thus it can report on the relative accessibility of cysteine residues within a protein. As a protein denatures, buried cysteine residues become accessible to CPM and the fluorescence signal increases. Purified Pgp (5 µg) was mixed with CPM (8 µg/ml) in a total volume of 200 µl. The reaction mixture was heated continuously from 10°C - 90°C in increments of 5°C for 2 minutes each. After 2 minutes at each temperature the fluorescence spectra was measured ($\lambda_{ex}$ 463±10 nm, $\lambda_{em}$ 410-560±20 nm) in a Perkin Elmer LS55 spectrophotometer. The fluorescence intensity (at 470 nm) at each time point was calculated as a % of the final fluorescence intensity. The assays were repeated twice for each sample.

Results & Discussion:

*Extraction of ABC transporters using SMA*

The initial aim was to determine if the SMALP method for extraction of membrane proteins could be successfully applied to eukaryotic ABC transporters. For each protein tested membrane fractions were prepared and mixed with 2.5% (w/v) SMA for 30-60 mins in the absence of any detergent, and insoluble material was removed by centrifugation. It can be seen in Figure 1 that for each of the proteins tested, Pgp, MRP1, MRP4, CFTR and ABCG2, successful extraction was observed using SMA. These samples included all of the commonly used cell types for eukaryotic ABC transporter expression, namely insect cells, mammalian cells and yeast. It also encompassed a range of sizes, with MRP1 at 190 kDa and comprising 17 transmembrane helices, being the largest, and both the conventional and reversed topology ABC transporters (i.e. ABCG2 having an NBD-TMD topology). The degree of extraction varied but there were no discernible patterns between expression systems or protein size.

For Pgp from High Five insect cells the extraction efficiency with SMA (60%) was comparable to previous reports using octyl-glucoside (50%) [20], and the extraction of MRP1 from H69AR cell membranes with SMA was comparable to previous reports using the detergent CHAPS (90%) [28].

MRP4 expressed in HEK cells is 63% solubilised by SMA whereas when expressed in Sf9 insect cells 86% is solubilised. The efficiency of MRP4 solubilisation with detergents has not previously been reported, therefore we also examined the ability of two commonly used detergents, octyl-glucuside and dodecymaltoside, to solubilise MRP4 from Sf9 cells (Supplementary Figure 1). Octyl glucoside was unable to solubilise MRP4 at all, whereas with DDM 78% of the MRP4 was successfully solubilised, which is comparable with the SMA. SMA solubilisation of ABCG2 from High Five insect cells was the least efficient at just 36%, however it was previously found that this protein is completely insoluble with most detergents and only the long chain foscholine detergents were capable of solubilising this protein at all [15]. One possible reason for the difficulty in solubilising ABCG2 from High Five cells may be the formation of large oligomers in this system [15], which are too large for the lipid discs formed by SMA. However the successful solubilisation of ABCG2 from both HEK cells and MCF7-FLV cells show that it is not a feature of ABCG2 *per se*. Interestingly the two most efficient extractions were from drug selected cancer cell lines (H69AR and MCF7-FLV) which overexpress transporters due to development of drug resistance. It is well known that such drug resistant cell lines display altered membrane constituents and properties [36-38], and it seems that this improves the ability of SMA to solubilise these transporters.

*Purification of ABC transporters encapsulated within SMALPs*

The SMA extracted membranes were then subjected to affinity purification. The SMALPs once formed are stable and, unlike detergent solubilised proteins, did not require addition of further polymer during the purification procedure. Figure 2 shows silver stained gels for the successful purification of each protein. The Pgp, MRP4, CFTR and ABCG2 proteins were purified using single step $Ni^{2+}$-NTA affinity chromatography, whereas MRP1 (which did not have a His-tag) was purified using a Protein A column and QCRL-1 antibody. An unexpected outcome of using SMA to solubilise the ABC transporters was a much higher degree of purity was obtained following just a single step affinity purification than has previously been observed with detergent solubilised proteins, which tend to require a second purification step of gel filtration [15, 21, 39] or ion exchange [40].

To ascertain whether this higher purity using SMA altered the final purified protein yield we quantified this and present the data in Supplementary Table 1. For purified Pgp obtained using SMA the yield was 631 ± 46 µg per litre of baculovirus infected High Five cell culture which is very

similar to that previously reported using octyl glucoside with these same cell membranes (792 ± 197 μg [20]), and the SMA purified Pgp is significantly more pure than the octyl glucoside preparation. Other reports which have used DDM to solubilise Pgp from these membranes have used a more stringent purification procedure including gel filtration as well as $Ni^{2+}$-NTA [41] and thus the Pgp produced was highly pure, however this resulted in a significantly lower yield (249 ± 15 μg/L culture) than that reported here with SMA. The yield of purified ABCG2 using SMA was 116 ± 32 μg/L culture, which is almost 3-fold higher than that previously obtained using foscholine (Supplementary Table S1, [15]). For MRP4 the yield of purified protein is relatively low at 35 ± 5 μg/L culture. This reflects a lower expression level in these cells, but it should be noted that the SMA allows an efficient extraction from these low expressing cells and an effective purification, whereas when using the detergent DDM with these same membranes the eluted fractions from the Ni-NTA column contain a large number of contaminating proteins in levels comparable or higher than the MRP4 (Supplementary Figure 3), showing that the SMA method is effective even for poorly expressed membrane proteins.

*Ligand binding by ABC transporters within SMALPs*

Next we determined whether the structure and function of the ABC transporters was retained following SMA extraction by investigating their ligand binding efficiency. A fluorescence quenching method devised by Liu & Sharom [29] was used to measure the binding of both doxorubicin (a transported substrate) and verapamil (a competitive inhibitor) to purified Pgp within SMALPs (Figure 3A). The data were best fitted by a single site binding curve with a $K_d$ for doxorubicin of 9.5 ± 1.5 μM (mean ± sem, n=3) and for verapamil $K_d$ = 2.0 ± 0.4 μM (mean ± sem, n = 4), which compare favourably to the previous results for detergent purified Pgp of 4.4 μM for doxorubicin and 2.4 μM for verapamil [29]. Furthermore the amplitude of the fluorescence change induced by drug binding shows that for both the SMA solubilised and previous detergent solubilised preparations the change in intensity for doxorubicin binding is close to twice that observed for verapamil [29], showing that the characteristics of doxorubicin and verapamil binding to SMALP-encapsulated Pgp are consistent with detergent solubilised Pgp.

The results of an estrone sulphate radioligand binding assay for SMA solubilised H69AR membranes in the absence or presence of GSH are shown in Figure 2. It has previously been shown that GSH binding causes a conformational change in MRP1 which increases the affinity for estrone sulphate binding [30]. SMALP-extracted MRP1 showed the same effect with the presence of 3 mM GSH causing a significant increase (2.3-fold, $P<0.05$) in the binding of estrone sulphate to SMALP encapsulated MRP1 which is comparable to that seen in native membranes.

A fluorescent chorophyll metabolite, Pheophorbide A, is a known substrate of ABCG2 [42]. Upon binding to SMALP encapsulated ABCG2 a large increase was detected in the emission fluorescence of pheophorbide A (Figure 3C & Supplementary figure S2A). This increase was dose-dependent (Figure 3C), specific to ABCG2 (Supplementary figure S2B) and could be displaced by the ABCG2 inhibitor chrysin (Figure 3C inset) with an $IC_{50}$ of 3.7 μM, which is comparable with previous reports [43].

*Nucleotide binding to purified Pgp encapsulated within SMALPs*

ABC transporters undergo nucleotide driven conformational changes to reorient substrate binding sites from high to low affinity conformations. For at least two of the transporters purified here it is ATP binding that provides this "power-stroke" [44, 45] and so we investigated whether the SMALP purified Pgp retained ATP binding. Figure 4 shows the quenching of intrinsic Pgp tryptophan fluorescence upon addition of either ATP or the fluorescent analogue TNP-ATP. The degree of tryptophan quenching and the affinity for TNP-ATP was much higher than for ATP itself, as has been reported previously [31,

46].The data were fit with a single site binding curve with a $K_d$ for ATP of 0.49 ± 0.08 mM and for TNP-ATP of 84 ± 9 μM, which are comparable to previously reported values of 0.28 mM for ATP and 50.6 μM for TNP-ATP [31].

*Biophysical characterisation of Pgp encapsulated within SMALPs*

Next we wanted to characterise the biophysical properties of the purified ABC-SMALPs. For these studies we used Pgp as an example, because it is one of the best characterized ABC transporters [41]. The CD spectra shown in Figure 5A shows that the purified Pgp is folded, and the characteristic minima at 208 nm and 222 nm show that the structure is predominantly α-helical, as expected from recent structural studies [47, 48]. Analytical ultracentrifugation (Figure 5B) gives a single major peak showing that the Pgp within the SMALPs is monomeric. This is also shown with the gel filtration in Figure 5C, where the main peak corresponds to a molecular weight of approx 164 kDa, in agreement with the predicted molecular weight (140 kDa unglycosylated). The gel filtration trace shows that the SMALP encapsulated Pgp does not show the levels of aggregation previously observed with dodecylmaltoside solubilised Pgp [39, 41].

Cryo-electron microscopy (Figure 6) shows discrete particles of 5nm width and 15 nm length, consistent with monomers of Pgp. Classification of >8000 selected particles showed that the majority of particles were probably monomeric with a few classes indicating two Pgp particles associating to form hinge-shaped particles (Figure 6B). An initial low resolution 3D structure (Figure 6C) produced from the single particles showed an envelope which was consistent with monomeric Pgp. Refinement of the structure (Figure 6D) was possible, generating a final (low) resolution of about 3.5nm (Figure 6E). The final structure was consistent with the published Pgp structure (3G5U) [49], although the resolution of the electron microscopy-derived structure did not allow unambiguous discrimination between the inward- and outward facing states (for example the outward-facing Sav1866 structure [50] could equally well be fitted within the low resolution envelope). Notably, the cryo-EM structure of Pgp within SMALPs lacks a large disc-shaped belt, which might have been expected. However we have observed previously that the polymer itself shows almost no signal in unstained cryo-EM samples. Secondly it suggests the disc does not contain a large belt of lipid molecules, just a small annulus, which agrees with a previous study showing approximately 11 lipid molecules per protein [17].

*Thermostability of Pgp encapsulated within SMALPs*

We surmised that the extraction of an ABC transporter with SMA, maintaining the lipid bilayer surrounding it, would not only preserve its structural integrity, but could also provide some advantages in terms of protein stability compared to detergent extraction. To investigate this we examined the thermostability of purified Pgp encapsulated within SMALPs and compared it to Pgp solubilized using octyl glucoside as previously published [20]. Thermostability was monitored using the method of Alexandrov *et al*. [35] where reactivity with the fluorophore CPM was monitored over time as the temperature was systematically increased (Figure 7). This demonstrates that the Pgp-SMALP sample was significantly more stable than the detergent solubilised sample, with the apparent melting temperature increasing by more than 10 °C.

*Conclusion*

Until now the solubilisation and purification of ABC transporters has relied on the use of detergents to disrupt the membrane environment surrounding membrane proteins. This study has demonstrated that the polymer SMA can instead be used to extract eukaryotic ABC transporters from a wide range of different cell types and expression systems without the need for detergents.

The extracted proteins retain the ability to bind substrates and nucleotide and can be purified by affinity chromatography. This is important for two key reasons: firstly detergents are expensive and the requirement to supplement all purification buffers with detergent to maintain solubility can become financially limiting when scaling up procedures. In contrast SMA is mass produced and can be used in a single step to form stable lipid disc structures that do not require addition of further polymer to any buffers. Secondly, and perhaps more importantly, the SMA method doesn't disrupt the lipid environment surrounding a membrane protein in the way that detergents do. Instead a segment of membrane is extracted, and the native lipid bilayer surrounding a membrane protein is maintained.

Furthermore the resultant purified transporters encapsulated within SMALPs are more pure, more stable and less prone to aggregation than detergent solubilised. It was also possible to concentrate the purified Pgp-SMALPs to > 8 mg/ml without significant loss of protein or aggregation.

In the current study we have not attempted to demonstrate ATPase of SMALP purified ABC transporters, (although we have showed that the proteins retain their interaction with nucleotide), because the SMALP is destabilised by divalent metal ions. Reconstitution from the lipid disc structure into proteoliposomes will be required to fully characterise the ATP hydrolysis kinetics and this will also allow the measurement of substrate transport.

However, as demonstrated by the work of Sligar and co-workers with nanodiscs, the small lipid-disc structure is amenable to many different techniques [51]. The amphipathic polymer-based SMALPs do not suffer from signal interference from the apolipoprotein surrounding the lipid disc. Finally the EM structural data shows that there is not a large belt of lipids, and thus it may be compatible with structural studies such as cryo-electron microscopy and in principle could be used in 3D crystallisation trials. Thus this work opens up several new opportunities for the structural and pharmacological study of ABC transporters, and their annular lipid environment.

Acknowledgements:

We thank Dr Richard Callaghan (Australian National University, Canberra, Australia) for providing insect cell membranes overexpressing Pgp or ABCG2, and Prof. Susan Cole (Queen's University, Kingston, ON, Canada) for providing H69AR cell pellets, pcDNA3.1-MRP1 plasmid and QCRL-1 antibody. MRP4 expression plasmid (pcDNA3.1-MRP4) was provided by Dr Dietrich Keppler (DKFZ, Heidelberg, Germany). We thank Dr David Poyner (Aston University) for advice and help with radioligand binding assays.

Funding:

AR was the recipient of a Royal Society Research Grant [RG110156], an ARCHA (Aston Research Centre for Health Aging) pump-priming grant and a Biochemical Society Guildford Bench Fund.
TD and MO thank the Biotechnology & Biological Sciences Research Council for funding [BB/J017310/1, BB/I020349/1, BB/G010412/1, BB/J010812/1, FoF/295].

References


1 Dean, M., Rzhetsky, A. and Allikmets, R. (2001) The human ATP-binding cassette (ABC) transporter superfamily. Genome Res. **11**, 1156-1166

2 Quazi, F. and Molday, R. S. (2011) Lipid transport by mammalian ABC proteins. Essays Biochem. **50**, 265-290

3 van de Ven, R., Oerlemans, R., van der Heijden, J. W., Scheffer, G. L., de Gruijl, T. D., Jansen, G. and Scheper, R. J. (2009) ABC drug transporters and immunity: novel therapeutic targets in autoimmunity and cancer. J. Leukocyte Biol. **86**, 1075-1087

4 Scherrmann, J. M. (2009) Transporters in absorption, distribution, and elimination. Chem. Biodivers. **6**, 1933-1942

5 Leslie, E. M., Deeley, R. G. and Cole, S. P. (2001) Toxicological relevance of the multidrug resistance protein 1, MRP1 (ABCC1) and related transporters. Toxicology. **167**, 3-23

6 Tamaki, A., Ierano, C., Szakacs, G., Robey, R. W. and Bates, S. E. (2011) The controversial role of ABC transporters in clinical oncology. Essays Biochem. **50**, 209-232

7 Kim Chiaw, P., Eckford, P. D. and Bear, C. E. (2011) Insights into the mechanisms underlying CFTR channel activity, the molecular basis for cystic fibrosis and strategies for therapy. Essays Biochem. **50**, 233-248

8 Kemp, S., Berger, J. and Aubourg, P. (2012) X-linked adrenoleukodystrophy: clinical, metabolic, genetic and pathophysiological aspects. BBA - Mol. Basis Dis. **1822**, 1465-1474

9 Rigaud, J. L. and Levy, D. (2003) Reconstitution of membrane proteins into liposomes. Methods Enzymol. **372**, 65-86

10 Bayburt, T. H. and Sligar, S. G. (2010) Membrane protein assembly into Nanodiscs. FEBS Letts.. **584**, 1721-1727

11 Alvarez, F. J., Orelle, C. and Davidson, A. L. (2010) Functional reconstitution of an ABC transporter in nanodiscs for use in electron paramagnetic resonance spectroscopy. J. Am. Chem. Soc. **132**, 9513-9515

12 Kawai, T., Caaveiro, J. M., Abe, R., Katagiri, T. and Tsumoto, K. (2011) Catalytic activity of MsbA reconstituted in nanodisc particles is modulated by remote interactions with the bilayer. FEBS Letts. **585**, 3533-3537

13 Ritchie, T. K., Kwon, H. and Atkins, W. M. (2011) Conformational analysis of human ATP-binding cassette transporter ABCB1 in lipid nanodiscs and inhibition by the antibodies MRK16 and UIC2. J. Biol. Chem. **286**, 39489-39496

14 Bao, H., Duong, F. and Chan, C. S. (2012) A step-by-step method for the reconstitution of an ABC transporter into nanodisc lipid particles. J. Vis. Exp., e3910

15 McDevitt, C. A., Collins, R. F., Conway, M., Modok, S., Storm, J., Kerr, I. D., Ford, R. C. and Callaghan, R. (2006) Purification and 3D structural analysis of oligomeric human multidrug transporter ABCG2. Structure. **14**, 1623-1632

16 Telbisz, A., Ozvegy-Laczka, C., Hegedus, T., Varadi, A. and Sarkadi, B. (2013) Effects of the lipid environment, cholesterol and bile acids on the function of the purified and reconstituted human ABCG2 protein. Biochem. J. **450**, 387-395

17 Knowles, T. J., Finka, R., Smith, C., Lin, Y. P., Dafforn, T. and Overduin, M. (2009) Membrane proteins solubilized intact in lipid containing nanoparticles bounded by styrene maleic acid copolymer. J. Am. Chem. Soc. **131**, 7484-7485

18 Jamshad, M., Lin, Y. P., Knowles, T. J., Parslow, R. A., Harris, C., Wheatley, M., Poyner, D. R., Bill, R. M., Thomas, O. R., Overduin, M. and Dafforn, T. R. (2011) Surfactant-free purification of membrane proteins with intact native membrane environment. Biochem. Soc. Trans. **39**, 813-818

19 Long, A. R., O'Brien, C. C., Malhotra, K., Schwall, C. T., Albert, A. D., Watts, A. and Alder, N. N. (2013) A detergent-free strategy for the reconstitution of active enzyme complexes from native biological membranes into nanoscale discs. BMC Biotechnol.. **13**, 41

20 Taylor, A. M., Storm, J., Soceneantu, L., Linton, K. J., Gabriel, M., Martin, C., Woodhouse, J., Blott, E., Higgins, C. F. and Callaghan, R. (2001) Detailed characterization of cysteine-less P-glycoprotein reveals subtle pharmacological differences in function from wild-type protein. Br. J. Pharmacol. **134**, 1609-1618

21 O'Ryan, L., Rimington, T., Cant, N. and Ford, R. C. (2012) Expression and purification of the cystic fibrosis transmembrane conductance regulator protein in Saccharomyces cerevisiae. J. Vis. Exp.61 pii: 3860
22 Cole, S. P., Bhardwaj, G., Gerlach, J. H., Mackie, J. E., Grant, C. E., Almquist, K. C., Stewart, A. J., Kurz, E. U., Duncan, A. M. and Deeley, R. G. (1992) Overexpression of a transporter gene in a multidrug-resistant human lung cancer cell line. Science. **258**, 1650-1654
23 Ito, K., Olsen, S. L., Qiu, W., Deeley, R. G. and Cole, S. P. (2001) Mutation of a single conserved tryptophan in multidrug resistance protein 1 (MRP1/ABCC1) results in loss of drug resistance and selective loss of organic anion transport. J. Biol. Chem. **276**, 15616-15624
24 Rivers, F., O'Brien, T. J. and Callaghan, R. (2008) Exploring the possible interaction between anti-epilepsy drugs and multidrug efflux pumps; in vitro observations. Eur. J. Pharmacol. **598**, 1-8
25 Haider, A. J., Briggs, D., Self, T. J., Chilvers, H. L., Holliday, N. D. and Kerr, I. D. (2011) Dimerization of ABCG2 analysed by bimolecular fluorescence complementation. PloS One. **6**, e25818
26 El-Sheikh, A. A., van den Heuvel, J. J., Krieger, E., Russel, F. G. and Koenderink, J. B. (2008) Functional role of arginine 375 in transmembrane helix 6 of multidrug resistance protein 4 (MRP4/ABCC4). Mol. Pharmacol. **74**, 964-971
27 Rius, M., Nies, A. T., Hummel-Eisenbeiss, J., Jedlitschky, G. and Keppler, D. (2003) Cotransport of reduced glutathione with bile salts by MRP4 (ABCC4) localized to the basolateral hepatocyte membrane. Hepatology. **38**, 374-384
28 Mao, Q., Leslie, E. M., Deeley, R. G. and Cole, S. P. (1999) ATPase activity of purified and reconstituted multidrug resistance protein MRP1 from drug-selected H69AR cells. BBA - Biomembranes. **1461**, 69-82
29 Liu, R. and Sharom, F. J. (1996) Site-directed fluorescence labeling of P-glycoprotein on cysteine residues in the nucleotide binding domains. Biochemistry. **35**, 11865-11873
30 Rothnie, A., Callaghan, R., Deeley, R. G. and Cole, S. P. (2006) Role of GSH in estrone sulfate binding and translocation by the multidrug resistance protein 1 (MRP1/ABCC1). The Journal of biological chemistry. **281**, 13906-13914
31 Liu, R., Siemiarczuk, A. and Sharom, F. J. (2000) Intrinsic fluorescence of the P-glycoprotein multidrug transporter: sensitivity of tryptophan residues to binding of drugs and nucleotides. Biochemistry. **39**, 14927-14938
32 Schuck, P. (2000) Size-distribution analysis of macromolecules by sedimentation velocity ultracentrifugation and lamm equation modeling. Biophysical journal. **78**, 1606-1619
33 Laue, T. M., Shah, B.D., Ridgeway, T.M. & Pelletier, S.L. . (1992) Computer-aided interpretation of analytical sedimentation data for proteins. . In Analytical ultracentrifugation in Biochemistry and Polymer Science (Harding, S. E., Rowe, A.J. & Horton, J.C., ed.). pp. 90-125, Royal Society of Chemistry, UK.
34 Tang, G., Peng, L., Baldwin, P. R., Mann, D. S., Jiang, W., Rees, I. and Ludtke, S. J. (2007) EMAN2: an extensible image processing suite for electron microscopy. J. Struct. Biol. **157**, 38-46
35 Alexandrov, A. I., Mileni, M., Chien, E. Y., Hanson, M. A. and Stevens, R. C. (2008) Microscale fluorescent thermal stability assay for membrane proteins. Structure. **16**, 351-359
36 Ramu, A., Glaubiger, D., Magrath, I. T. and Joshi, A. (1983) Plasma membrane lipid structural order in doxorubicin-sensitive and -resistant P388 cells. Cancer Res. **43**, 5533-5537
37 May, G. L., Wright, L. C., Dyne, M., Mackinnon, W. B., Fox, R. M. and Mountford, C. E. (1988) Plasma membrane lipid composition of vinblastine sensitive and resistant human leukaemic lymphoblasts. International journal of cancer. J. Intl. Cancer. **42**, 728-733
38 Tapiero, H., Mishal, Z., Wioland, M., Silber, A., Fourcade, A. and Zwingelstein, G. (1986) Changes in biophysical parameters and in phospholipid composition associated with resistance to doxorubicin. Anticancer Res. **6**, 649-652
39 McDevitt, C. A., Shintre, C. A., Grossmann, J. G., Pollock, N. L., Prince, S. M., Callaghan, R. and Ford, R. C. (2008) Structural insights into P-glycoprotein (ABCB1) by small angle X-ray scattering and electron crystallography. FEBS Letts. **582**, 2950-2956
40 Lerner-Marmarosh, N., Gimi, K., Urbatsch, I. L., Gros, P. and Senior, A. E. (1999) Large scale purification of detergent-soluble P-glycoprotein from Pichia pastoris cells and characterization of

nucleotide binding properties of wild-type, Walker A, and Walker B mutant proteins. J. Biol. Chem. **274**, 34711-34718
41 Pollock, N. L., McDevitt, C. A., Collins, R., Niesten, P. H., Prince, S., Kerr, I. D., Ford, R. C. and Callaghan, R. (2013) Improving the stability and function of purified abcb1 and abca4: The influence of membrane lipids. BBA - Biomembranes **134,** 134-147
42 Robey, R. W., Steadman, K., Polgar, O., Morisaki, K., Blayney, M., Mistry, P. and Bates, S. E. (2004) Pheophorbide a is a specific probe for ABCG2 function and inhibition. Cancer Res. **64**, 1242-1246
43 Zhang, S., Yang, X. and Morris, M. E. (2004) Flavonoids are inhibitors of breast cancer resistance protein (ABCG2)-mediated transport. Mol. Pharmacol. **65**, 1208-1216
44 McDevitt, C. A., Crowley, E., Hobbs, G., Starr, K. J., Kerr, I. D. and Callaghan, R. (2008) Is ATP binding responsible for initiating drug translocation by the multidrug transporter ABCG2? FEBS J. **275**, 4354-4362
45 Martin, C., Berridge, G., Mistry, P., Higgins, C., Charlton, P. and Callaghan, R. (2000) Drug binding sites on P-glycoprotein are altered by ATP binding prior to nucleotide hydrolysis. Biochemistry. **39**, 11901-11906
46 Liu, R. and Sharom, F. J. (1997) Fluorescence studies on the nucleotide binding domains of the P-glycoprotein multidrug transporter. Biochemistry. **36**, 2836-2843
47 Jin, M. S., Oldham, M. L., Zhang, Q. and Chen, J. (2012) Crystal structure of the multidrug transporter P-glycoprotein from Caenorhabditis elegans. Nature. **490**, 566-569
48 Ward, A. B., Szewczyk, P., Grimard, V., Lee, C. W., Martinez, L., Doshi, R., Caya, A., Villaluz, M., Pardon, E., Cregger, C., Swartz, D. J., Falson, P. G., Urbatsch, I. L., Govaerts, C., Steyaert, J. and Chang, G. (2013) Structures of P-glycoprotein reveal its conformational flexibility and an epitope on the nucleotide-binding domain. Proc. Natl Acad. Sci. USA. **110**, 13386-13391
49 Aller, S. G., Yu, J., Ward, A., Weng, Y., Chittaboina, S., Zhuo, R., Harrell, P. M., Trinh, Y. T., Zhang, Q., Urbatsch, I. L. and Chang, G. (2009) Structure of P-glycoprotein reveals a molecular basis for poly-specific drug binding. Science. **323**, 1718-1722
50 Dawson, R. J. and Locher, K. P. (2006) Structure of a bacterial multidrug ABC transporter. Nature. **443**, 180-185
51 Schuler, M. A., Denisov, I. G. and Sligar, S. G. (2013) Nanodiscs as a new tool to examine lipid-protein interactions. Methods Mol Biol. **974**, 415-433

Figure legends:

**Figure 1. Extraction of ABC transporters using SMA polymer.** Membrane preparations (30 mg/ml wet weight) were mixed with 2.5 %(w/v) SMA in 20 mM Tris pH8, 150 mM NaCl, 10 %(v/v) glycerol for 1 hour at room temperature, then centrifuged at 100,000 g for 20 min. Sample F also had 1 %(w/v) DMPC added alongside the SMA, and was incubated at 37°C rather than room temperature. Samples of the soluble and insoluble material were assayed by Western blotting, and the percentage of the target protein in each was measured using densitometry.

**Figure 2. Purification of ABC transporters within SMA-lipid particles.** A; SMA solubilised Pgp membranes (Sol) were incubated with Ni-NTA resin at 4°C overnight. Unbound material (FT) was removed and the resin was washed with buffer supplemented with 20-60mM imidazole before being eluted with buffer containing 120mM imidazole. Samples from each fraction were run on SDS-PAGE and silver stained. B-D; elution fractions from purifications carried out as in A but for ABCG2 (B), MRP4 (C) and CFTR (D). E; QCRL-1 antibody was bound to a protein A column, then SMA solubilised H69AR membranes were incubated with the column for 30 min at 20°C. Unbound proteins were washed out and MRP1 was eluted upon addition of the peptide SSYSGDI.

**Figure 3. Ligand binding assays.** A; Purified Pgp-SMALPs were labelled with the fluorophore MIANS, then fluoresecence quenching upon binding of the inhibitor verapamil (open circles) and transport substrate doxorubicin (closed circles) were measured. B; Binding of $^{3}$H-estrone sulphate to SMA solubilised H69AR membranes (MRP1) was measured in the presence and absence of 3mM GSH (*P<0.05). E; Specific binding of pheophorbide A to SMA-solubilised HEK-ABCG2 membranes detected by an enhanced fluorescence of pheophorbide A at 681 nm. All data are mean±sem, n≥3. Inset; dose-dependent displacement of pheophorbide A binding by chrysin.

**Figure 4. Nucleotide binding to purified Pgp-SMALPs.** Quenching of the intrinsic tryptophan fluorescence of purified Pgp (50µg/ml) within SMALPs upon binding of nucleotides (A) ATP and (B) TNP-ATP. Data are mean±sem and n≥3.

**Figure 5. Biophysical characterisation of purified Pgp-SMALPs.** A; Circular dichroism spectra at 0.65 mg/ml with a 0.1mm pathlength. B; Analytical ultracentrifugation trace. C; Gel filtration on a superdex 200 column (diameter 1.6cm, height 55cm), solid line is absorbance at 280nm, dashed line is conductivity.

**Figure 6. Structural characterisation of purified Pgp-SMALPs.** A; Pgp particles solubilised in SMALPs and visualised (unstained) using cryo-electron microscopy. The edge of the hole in the carbon support film of the electron microscopy grid is visible top right. The particles are 10-15nm diameter and are relatively monodisperse. B; Classification of the particles reveals elongated particles of about 5nm width and 15nm length. Some classes appear to be formed by two particles associating. Box size is 21.6nm. C; An initial low resolution 3D envelope generated from single particle classes, and D; further refinement of the structure against all the raw particles. Orthogonal views are shown, with the ABCB1 crystal structure (3G5U) docked within it (blue ribbon). The refined structure was estimated to be at about 3.5nm resolution (E).

**Figure 7. Thermostability of purified Pgp.** Purified Pgp (5 µg) was mixed with 8 µg/ml coumarin maleimide in a total volume of 200 µl The reaction mixture was heated continuously from 10°C - 90°C in increments of 5°C for 2 minutes each and the fluorescence spectra measured.

Fluorescence intensity (at 470nm) at each time point was calculated as a % of the final fluorescence intensity. Pgp was either solubilised with 2.5% SMA (open circles) or 2% octyl glucoside (closed circles).

Figure 1

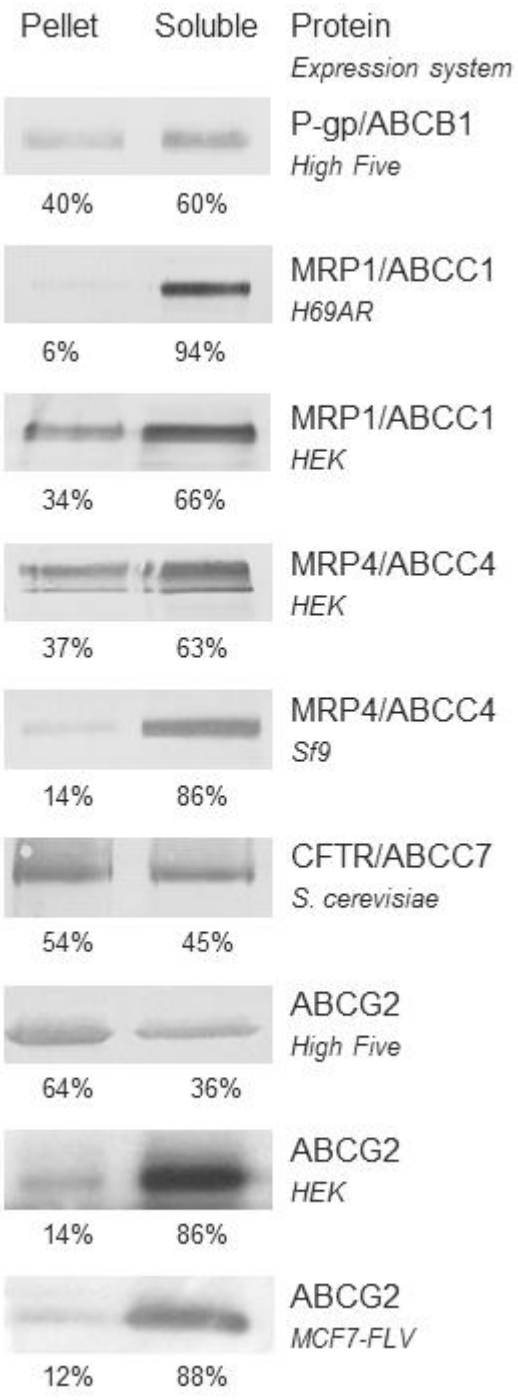
Pellet
Soluble
Protein
Expression system
P-gp/ABCB1
High Five
40%
60%
MRP1/ABCC1
H69AR
6%
94%
MRP1/ABCC1
HEK
34%
66%
MRP4/ABCC4
HEK
37%
63%
MRP4/ABCC4
Sf9
14%
86%
CFTR/ABCC7
S. cerevisiae
54%
45%
ABCG2
High Five
64%
36%
ABCG2
HEK
14%
86%
ABCG2
MCF7-FLV
12%
88%

Figure 2

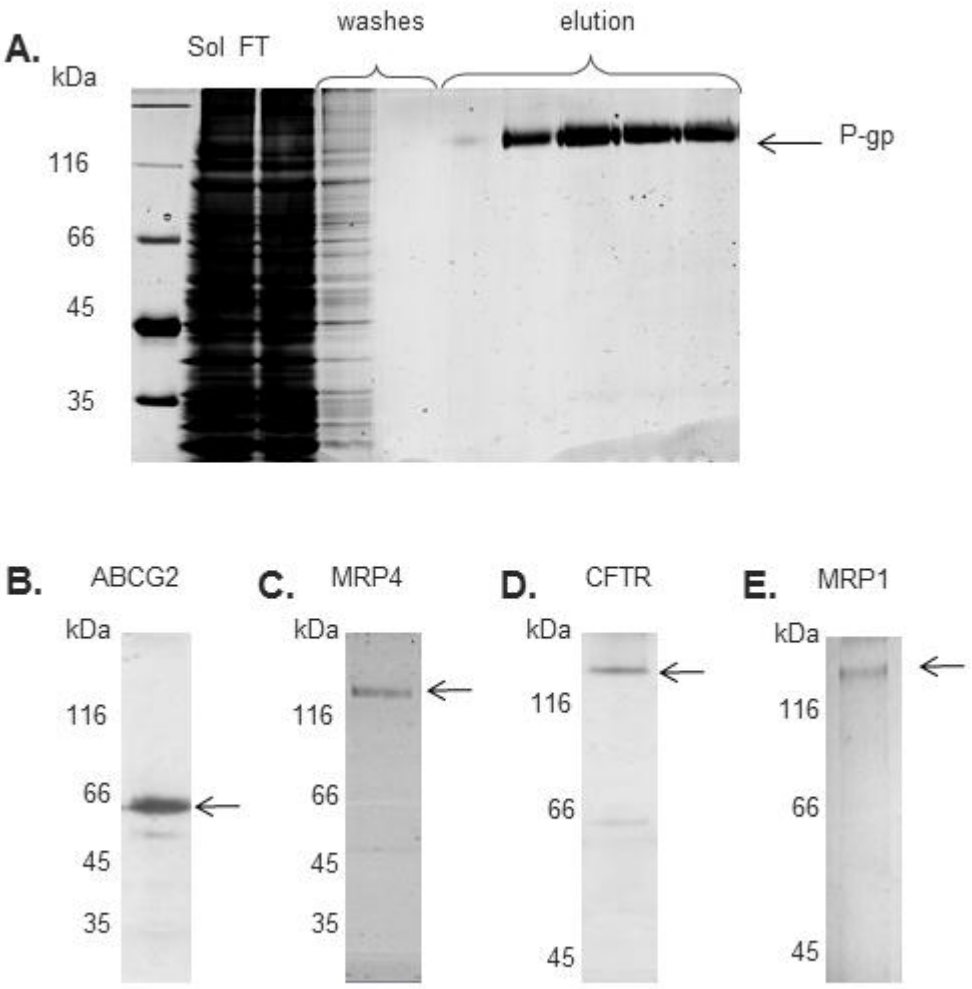
A.
Sol FT
washes
elution
kDa
116
66
45
35
P-gp
B.
ABCG2
C.
MRP4
D.
CFTR
E.
MRP1

Figure 3

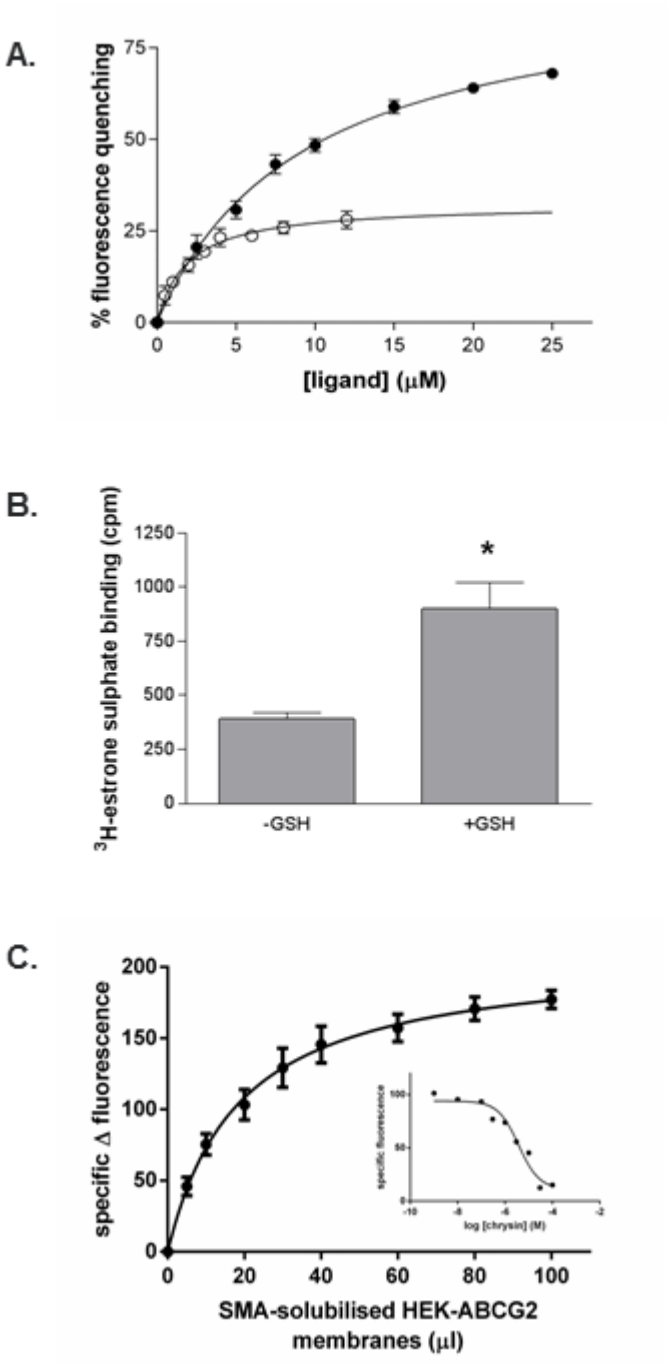
A.
% fluorescence quenching
75
50
25
0
0
5
10
15
20
25
[ligand] (μM)
B.
$^3$H-estrone sulphate binding (cpm)
1250
1000
750
500
250
0
*
-GSH
+GSH
C.
specific Δ fluorescence
200
150
100
50
0
0
20
40
60
80
100
SMA-solubilised HEK-ABCG2 membranes (μl)
specific fluorescence
log [chrysin] (M)

Figure 4

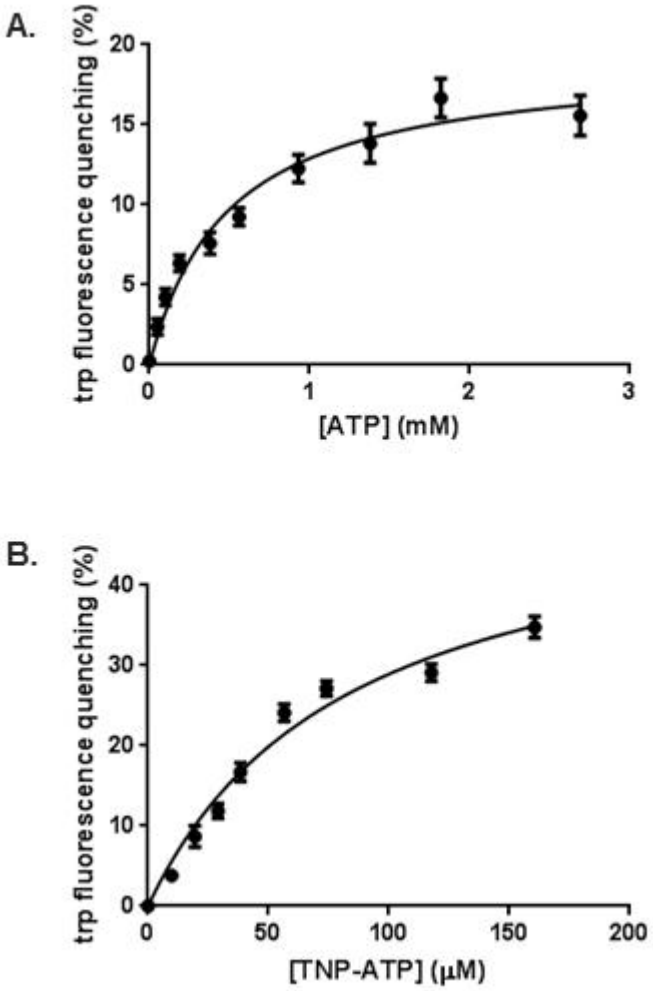
A.
trp fluorescence quenching (%)
20
15
10
5
0
0
1
2
3
[ATP] (mM)
B.
trp fluorescence quenching (%)
40
30
20
10
0
0
50
100
150
200
[TNP-ATP] (μM)

Figure 5

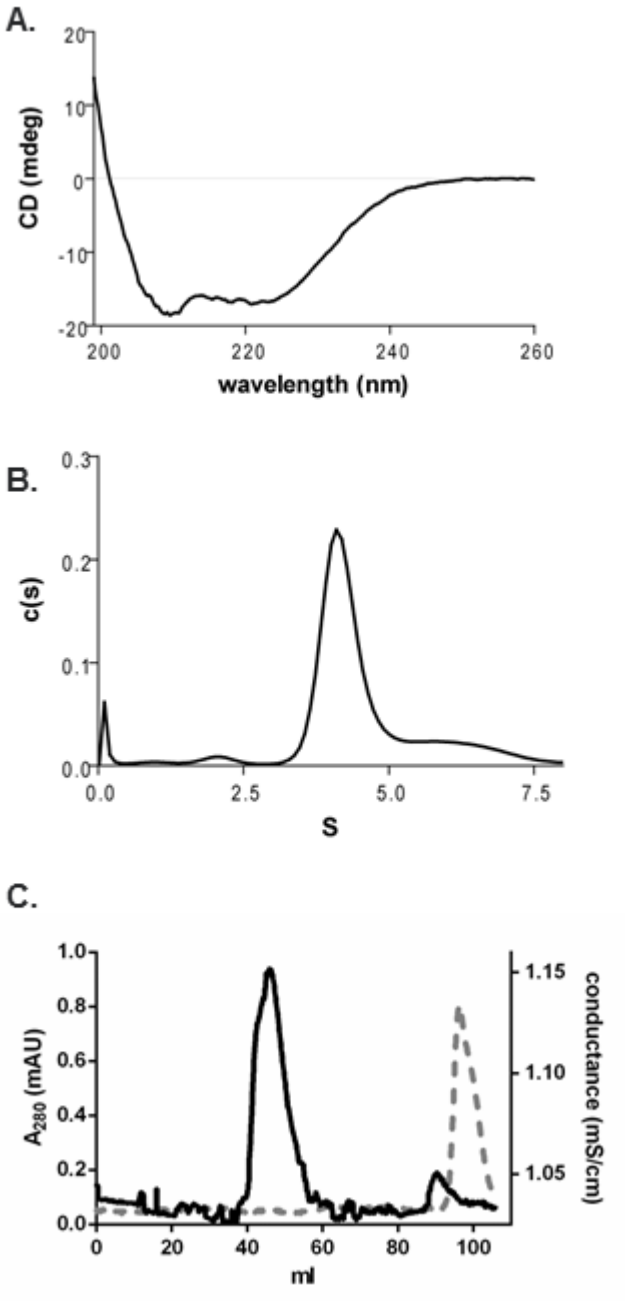
A.
CD (mdeg)
20
10
0
-10
-20
200
220
240
260
wavelength (nm)
B.
c(s)
0.3
0.2
0.1
0.0
0.0
2.5
5.0
7.5
S
C.
A280 (mAU)
1.0
0.8
0.6
0.4
0.2
0.0
conductance (mS/cm)
1.15
1.10
1.05
0
20
40
60
80
100
ml

Figure 6

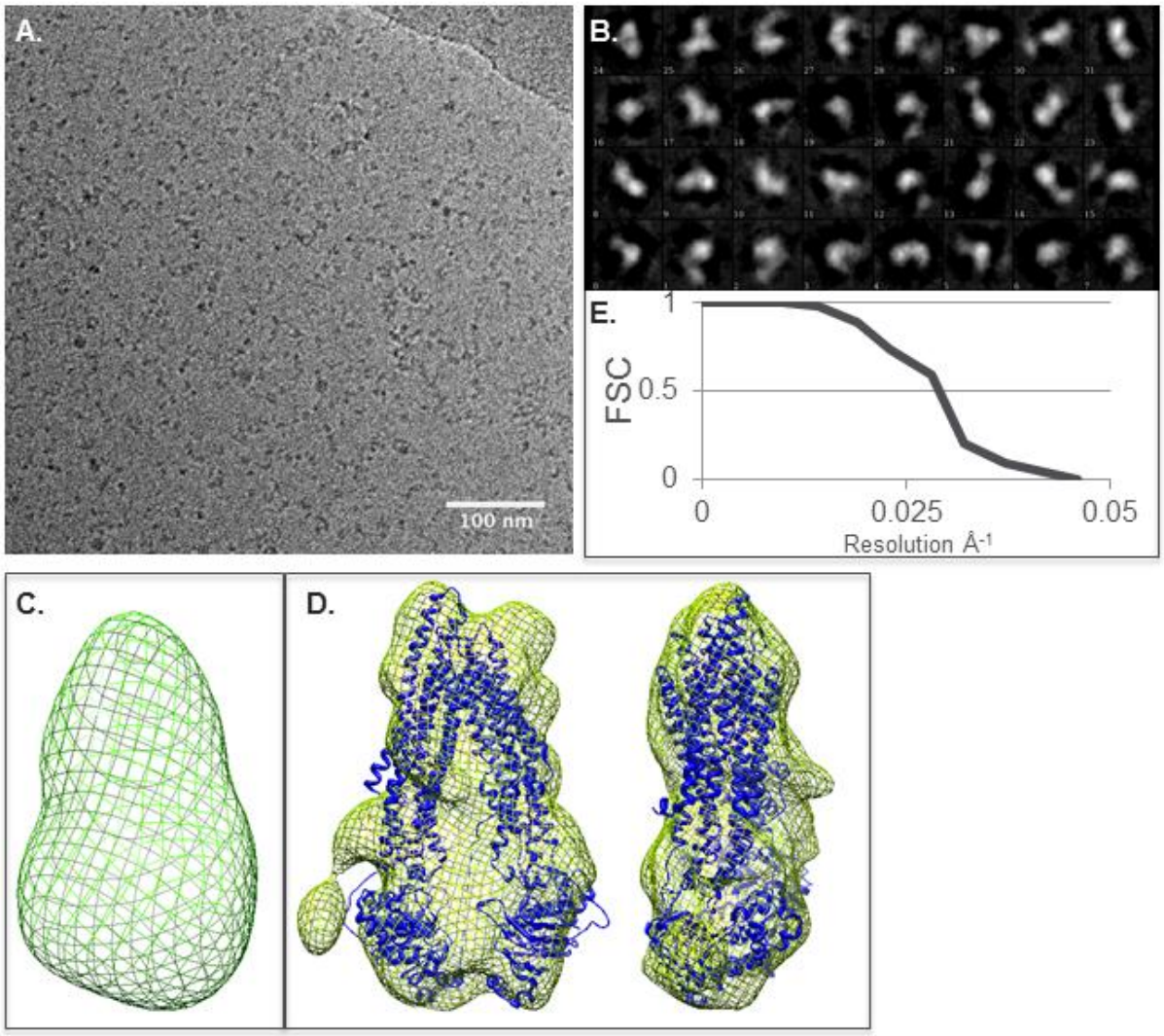

Figure 7

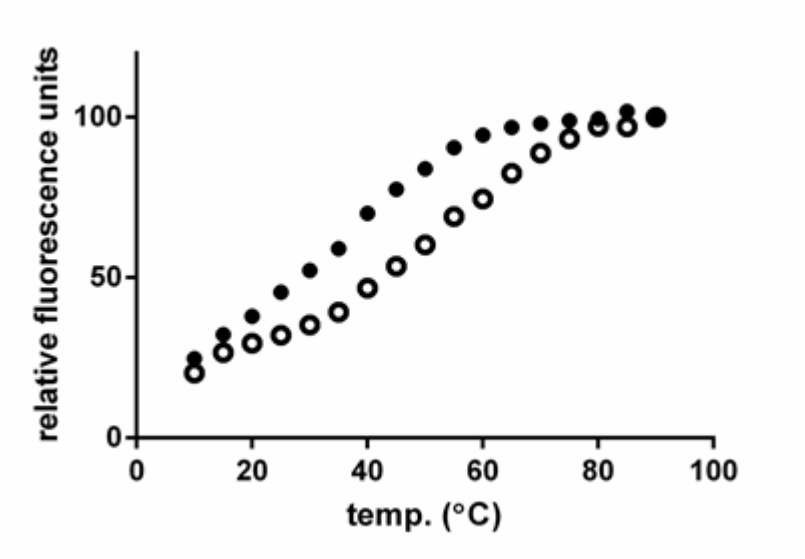

# Supplementary Information

| **ABC protein** (*expression cell type*) | Yield of purified protein (µg) per 1L culture | | |
|---|---|---|---|
| | SMA | detergents | |
| | | OG[a] | DDM[b] |
| **Pgp/ABCB1** (*High Five*) | 631 ± 46 | 792 ± 197 | 249 ± 15 |
| | | FC-16[c] | |
| **ABCG2** (*High Five*) | 116 ± 32 | 39 ± 14 | - |
| **MRP4/ABCC1** (*Sf9*) | 35 ± 3 | - | - |
| | | DDM[d] | LPG[d] |
| **CFTR/ABCC7** (*S.cerevisiae*) | 33 | 67 | 133 |
| | Yield of purified protein (µg) per $10^8$ cells | | |
| | | CHAPS[e] | |
| **MRP1/ABCC1** (*H69AR*) | 126 | 250 | - |

**Supplementary Table S1. Comparison of yield of purified protein using SMA or detergents**
The final yield of purified protein produced using SMA was calculated for each of the proteins studied per litre of cultured cells (Pgp, ABCG2, MRP4 and CFTR) or per $10^8$ cells (MRP1). Where errors are shown data are mean±sem, n≥3. For comparison yields previously obtained with these membranes using various different detergents are also shown. OG (octyl –β-D-glucoside), DDM (dodecyl-β-D- maltoside), FC-16 (foscholine-16), LPG (lysophosphatidylglycerol), CHAPS (3-(3-cholamidopropyl)dimethylammonio-1-propanesulfonate).

[a]Taylor *et al* (2001) Br J Pharmacol 134;1609-1618, R. Callaghan (personal communication)
[b]Pollock *et al* (2014) Biochim Biophys Acta 1838;134-47, R. Callaghan (personal communication)
[c]McDeviit *et al* (2006) Structure 14;1623-32, R. Callaghan (personal communication)
[d]O'Ryan *et al* (2012) J Vis Exp 61, e3860, doi:10.3791-3860
[e]Mao *et al* (1999) Biochim Biophys Acta 1461;69-82.

# Supplementary Figure 1

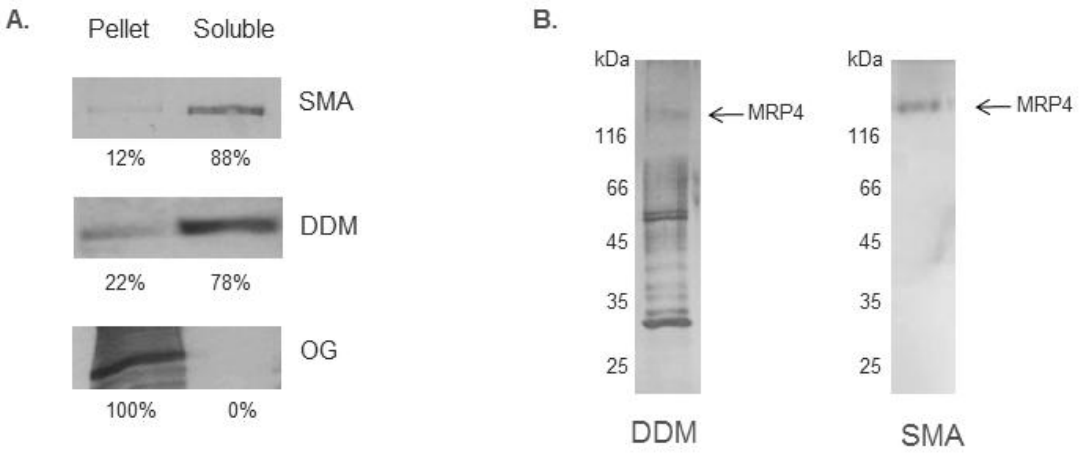


**Figure S1. Comparison of MRP4 solubilisation and purification from Sf9 cells using SMA or detergent.**A. Sf9-MRP4 membranes were solubilised in either 2.5 %(w/v) SMA, 2 %(w/v) DDM or 2 %(w/v) OG for 1 hour and then centrifuged at 100,000g for 20min at 4°C. Samples of the soluble and insoluble material were assayed by Western blotting, and the percentage of the target protein in each was measured using densitometry. B. Soluble material was incubated with Ni-NTA resin overnight at 4°C, transferred to a mini column and washed extensively with buffer supplemented with 20mM imidazole. Samples shown were eluted using 120mM imidazole. SDS-PAGE gels are silver stained.

# Supplementary Figure 2

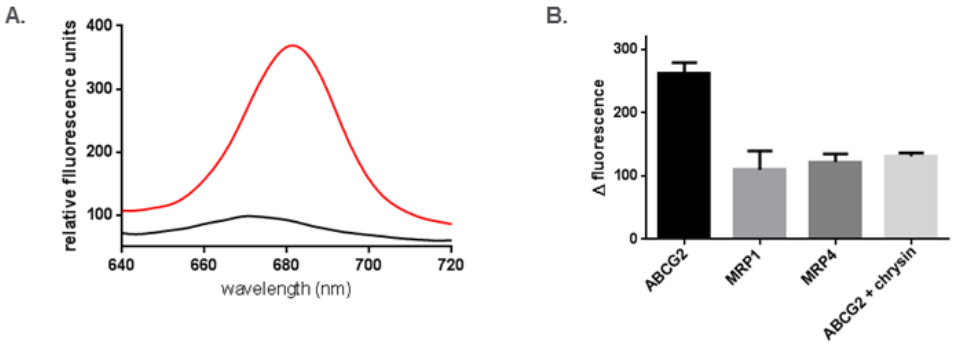


**Figure S2. Enhanced fluorescence of pheophorbide A upon binding to ABCG2.** A; Pheophorbide A (10 µM, 1 ml) fluorescence with an excitation wavelength of 390±10 nm, before (black) and after (red) a 10 minute incubation with ABCG2 containing SMA-solubilised membranes (40 µl). B; The increase in fluorescence emission at 681 nm of pheophorbide A (as in A) when SMA-solubilised membranes with overexpressed ABCG2, MRP1 or MRP4 are added, or when ABCG2 membranes are preincubated for 10 minutes with 30 µM chrysin. Data are mean±sem, n≥3.